LAWRENCE
LIVERMORE
NATIONAL
LABORATORY

LLNL-JRNL-431877

National Ignition Facility (NIF) Neutron time-of-flight (nTOF) Measurements

R. A. Lerche, V. Y. Glebov, M. J. Moran, J. M. McNaney, J. D. Kilkenny, M. Eckart, R. A. Zacharias, J. J. Haslam, T. J. Clancy, M. F. Yeoman, D. P. Warwas, T. C. Sangster, C. Stoeckl, J. Knauer, C. J. Horsfield

May 14, 2010

Review of Scientific Instruments

Disclaimer

National Ignition Facility (NIF) neutron time-of-flight (nTOF) measurements[a)]

R. A. Lerche,[1,b)] V. Yu. Glebov,[2] M. J. Moran,[1] J. M. McNaney,[1] J. D. Kilkenny,[1]
M. J. Eckart,[1] R. A. Zacharias,[1] J. J. Haslam,[1] T. J. Clancy,[1] M. F. Yeoman,[1] D. P. Warwas,[1]
T. C. Sangster,[2] C. Stoeckl,[2] J. P. Knauer[2] and C. J. Horsfield[3]

[1]*Lawrence Livermore National Laboratory, P. O. Box 808, Livermore, California 94551, USA*
[2]*Laboratory for Laser Energetics, University of Rochester, Rochester, New York 14623-1299, USA*
[3]*Atomic Weapons Establishment, Aldermaston, Reading, Berkshire, RG7 4PR, U.K.*

(Presented XXXXX; received XXXXX; accepted XXXXX; published online XXXXX)
(Dates appearing here are provided by the Editorial Office)

The first three of eighteen neutron time-of-flight (nTOF) channels have been installed at the National Ignition Facility (NIF). The role of these detectors includes yield, temperature, and bang time measurements. This article focuses on nTOF data analysis and quality of results obtained for the first set of experiments to use all 192 NIF beams. Targets produced up to $2x10^{10}$ 2.45-MeV neutrons for initial testing of the nTOF detectors. Differences in neutron scattering at the OMEGA laser facility where the detectors were calibrated and at NIF result in different response functions at the two facilities. Monte Carlo modeling shows this difference. The nTOF performance on these early experiments indicates the nTOF system with its full complement of detectors should perform well in future measurements of yield, temperature, and bang time.

I. INTRODUCTION

Three channels of an eighteen-channel neutron time-of-flight (nTOF) system[1] have been installed at the National Ignition Facility[2] (NIF). During the fall of 2009, they recorded data on the first series of shots that used all 192 NIF beams. Targets were designed to check and tune Hohlraum energetics in preparation for the coming ignition campaign.[3] Laser and target parameters were scaled to create plasma conditions similar to that of a 1.2-MJ ignition Hohlraum using 500–750 kJ of laser energy. Target capsules were filled with 8.3 mg/cm^3 of helium gas to generate x rays at the time of peak convergence (bang time). While neutron production was not a goal for these experiments, some of the target capsules were filled with 7%-10% deuterium to produce a limited number of 2.45-MeV fusion neutrons. This permitted initial testing of the most sensitive of the nTOF detectors. Two of the detectors are nearly identical. This article, describes the initial measurements made with these two detectors. By comparing the results from two independent detectors, measurement precision is demonstrated.

The eighteen nTOF channels are designed to measure yield, ion temperature, bang time, and down-scattered fraction over a wide range of neutron yields.[4] The initial three detectors were designed to make measurements for low yield NIF targets. Before their installation at the NIF, they were calibrated at the University of Rochester's OMEGA laser facility. For the first series of NIF shots, these detectors took on the role of measuring three target quantities: neutron yield, ion temperature, and bang time. By using these first nTOF detectors for three measurements instead of just one, NIF scientists and engineers gained valuable operating experience with the new detectors at the new facility. At earlier inertial confinement fusion (ICF) facilities these three tasks were normally done with three separate systems employing similar detectors. Yield measurements are the least demanding as yield is simply proportional to the signal integral. Temperature measurements ideally use a longer flight path so that the neutron temporal spread can be more easily separated from the detector response.[5] For bang time measurements, short flight paths are preferable to minimize neutron temporal spreading at the detector and thus minimize the error in determining the neutron arrival time at the detector.[6] Successful measurements were made for each quantity and point to successful measurements when the full complement of nTOF detectors is available.

This article begins with a brief history of nTOF systems traditionally used to measure ion temperatures at LLNL inertial confinement fusion (ICF) facilities, and the similarity of these detectors to those used for measuring neutron yield and bang time. This is followed by a description of the NIF 4.5-meter nTOF detectors, their calibration at OMEGA, and their use at NIF. A significant portion of the article is devoted to understanding detector response functions and the differences between the OMEGA and NIF environments. The results of the three measurements are presented along with a brief discussion of the expectations for future measurements.

II. nTOF HISTORY

In 1973 Brysk[7] published the currently accepted distribution function for the neutron energy spectra of fusion neutrons emitted from deuterium and deuterium-tritium plasmas having a Maxwellian distribution. He found the energy spectra of the initially mono-energetic neutrons to be Gaussian with a width proportional to the square root of the ion temperature. The mono-energetic nature of the neutrons and the short burn duration[8] (~100 ps) and small emitting region[9] (<100-um dia) of an ICF capsule makes neutron time-of-flight an ideal technique for measuring the plasma ion temperature. The first ICF nTOF ion temperature measurements at LLNL were made at the Argus laser facility.[10]

The nTOF systems at the Argus and Shiva laser facilities had long, well collimated, dual flight paths, 45 and 120 meters, respectively. Long flight paths were necessary because of the

[a)] Invited paper published as part of the Proceedings of the 18th Topical Conference on High-Temperature Plasma Diagnostics, Wildwood, New Jersey, May, 2010.
[b)] Electonic mail: lerche1@llnl.gov.

relatively slow time response of available detectors. Neutron-to-light conversion took place in large 8" diameter, 4" thick plastic scintillators optically coupled to XP2020 photomultiplier tubes (PMTs). Transit time for DT neutrons through the scintillator was ~2 ns, about half the PMT's 3.5-ns full-width at half-maximum (FWHM) response. Both systems were used only with 14-MeV neutrons from deuterium-tritium (DT) reactions. Neutrons scattered from the target chamber were prevented from reaching the detectors by collimation and shield walls. No shielding was placed directly between the target and detector or around the detector. Neutron yields at both facilities were measured with similar scintillator/PMT detectors placed only a few meters from the target chamber and by copper activation.

Microchannel-plate photomultiplier tubes (MCP/PMT) were available when LLNL's Nova facility came online in the 1980s.[6] Their 350-450 ps (FWHM) response allowed two significant nTOF system design changes: a smaller, faster detector package and a correspondingly shorter flight path. Initially, quenched 4.6-cm diameter, 2.5-cm thick BC-422Q scintillators were optically coupled to MCP/PMTs and read out with 500-MHz oscilloscopes. The detector components were well matched to each other: DT neutron transit time through the scintillator 500 ps, scintillator decay rate 700 ps, PMT response 450 ps FWHM, and scope response 700 ps to give an overall detector response of about 1 ns. The initial Nova nTOF system had an 18 m flight path with the detector about 8 m outside the target bay. A hole through the concrete target room shield wall provided reasonable collimation.

After Nova operations began, another significant event took place. Additional fast nTOF nTOF detectors were installed, one at ~8 m and another at ~4 m. These detectors allowed measuring ion temperature with 2.45-MeV (DD) neutrons from lower yield, deuterium filled targets. These detectors were located inside the Nova target room and used without collimation. Besides detecting neutrons coming directly from the target, these detectors also recorded signals from scattered neutrons. The tail of the 4-meter detector signal included neutrons scattered from the target chamber, the tail of the 8-meter detector signal included neutrons back-scattered from the concrete shield wall immediately behind the detector. nTOF detectors at the OMEGA laser facility are also located within that facility's target room and are operated without collimation.

At LLNL and OMEGA scintillator/PMT detectors are also used to measure neutron yield and bang time. At early LLNL facilities yield detectors were too close to the target and to slow to measure temperature. Absolute neutron yields were determined primarily by copper activation for DT neutrons and indium activation for DD neutrons. nTOF detectors can provide good DD and DT yield measurements once they are calibrated. OMEGA routinely uses them to measure target neutron yields. Bang time, the time when neutrons are emitted from the target, is another measurement made with fast neutron detectors. For these measurements the target-to-detector distance is kept short (50 cm) and thin quenched scintillators are used to keep time spread to a minimum. More recently, fast CVD diamond detectors have become available for nTOF measurements.[11]

III. NIF nTOF DETECTORS

The first three nTOF detectors installed at NIF are similar. These detectors were designed to measure neutron yields from low yield targets. The two detectors used in this study each use a 2-cm thick by 4-cm dia BC-422 plastic scintillator as the neutron-to-light converter. A Photek PMT240 MCP PMT collects the light and produces a current pulse that is recorded with a 1-GHz,

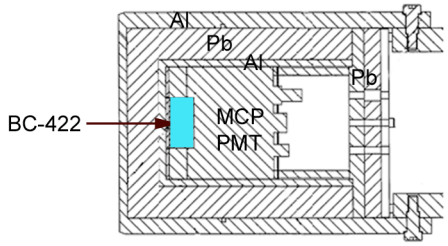

FIG. 1. Plastic scintillator, PMT and lead x-ray shielding.

10-GS/s, Tektronix DPO7104 digital oscilloscope. Each detector is connected to the oscilloscope via ~100 feet of LMR400, ~12 feet of RG142, and 10 ft of LMR195U cable. At the oscilloscope, a power splitter divides the signal 4 ways so that it can be recorded by each of the oscilloscope's four channels. By applying different attenuators and voltage settings to the 4 channels, a wider range of signal amplitudes can be covered. Each detector is placed inside a lead pig (Fig. 1) that provides shielding against target emitted x rays. The lead shielding is 1-inch thick all the way around the detector. Each lead pig is mounted inside a separate reentrant well at a NIF target chamber port (Fig. 2). This allows each detector to be far enough inside the target chamber wall that complications of neutron backscatter are avoided while remaining outside the chamber vacuum.

One detector reported in this article was calibrated at the Omega laser facility; the other detector was calibrated at NIF using the calibrated detector as the reference. At OMEGA the detectors being calibrated are operated in a configuration that mimics their usage at NIF: same cables, same oscilloscopes, similar distances from target chamber center (TCC), similar DD neutron yields, and similar ion temperatures. Yield and temperature measurements made with standard OMEGA nTOF detectors operated on the same shots are used to determine the calibration for the new detectors intended for NIF use. The detectors are placed outside the 1.7-meter radius target chamber with the plastic scintillator 5.2 m from TCC. A 13-mm thick aluminum window along the neutron flight path separates the chamber vacuum from the outside air and allows passage of the neutrons with little attenuation. Exploding pusher targets produce 10^8 to 10^{10} DD neutrons with plasma temperatures of 2-3 keV. Fit parameters describing the detector prompt (impulse) response

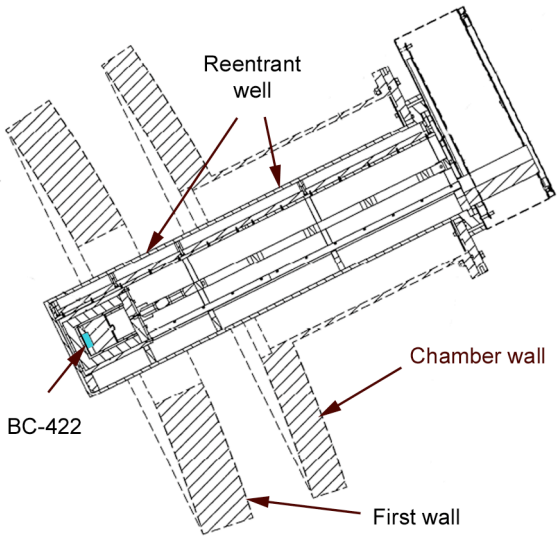

FIG 2. nTOF detector with lead shielding mounted in a reentrant well at a NIF diagnostic port.

function (PRF) are determined by an analysis method described by Murphy[12] using temperatures measured with the OMEGA facility's 12-m nTOF detector.

The scattering environment of the two facilities is different. At NIF the scintillator sits 4.58-cm from TCC. Scattering from the reentrant aluminum well that holds the detector and scattering from the low density, louvered NIF "first wall" at ~4.6 m from TCC add to the recorded signal. Unlike OMEGA, the scintillator is inside the NIF target chamber wall by ~40 cm, DD neutrons backscattered from the wall arrive well after the signal of interest. An understanding of the Omega calibration data is fundamental to interpreting NIF data.

IV. PROMPT RESPONSE FUNCTION (PRF)

Correct interpretation of data recorded at NIF and OMEGA requires knowledge of the PRF at both facilities. In this article, the PRF is defined as the average system response per source neutron. It can be thought of as the convolution of three elements: the energy deposition rate in the plastic scintillator, the decay rate of the plastic scintillator, and the response of the recording system made up of the PMT, connecting cables, and oscilloscope. This represents the average PRF per source neutron, not the PRF of an individual neutron. The scintillator decay and the recording system components of the PRF are the same at NIF and OMEGA. Because of the different scattering environments, the neutron energy deposition rate in the scintillator differs between the two facilities.

Monte Carlo calculations[13] estimated energy deposition rates. Calculations assumed simple models for the detector and for the OMEGA and NIF target chamber geometries (see Fig. 3). Detector and lead pig were modeled as a scintillator surrounded by a lead cylinder with an aluminum liner and outer container. The OMEGA target chamber was modeled as a 3-inch thick, 1.7-m radius aluminum sphere. Between TCC and the detector, there is a 13-mm thick aluminum window. The detector and lead pig were placed with the scintillator 5.2 m from TCC, the OMEGA calibration distance. For NIF calculations the detector and lead pig were placed inside a reentrant aluminum well with the scintillator 4.58 m from TCC. Since backscatter from the NIF chamber wall arrives outside the time window of interest, it is not included in the calculation. Energy deposition is tracked in 100-ps steps over a 40 ns window. Results are shown in Fig. 4. The figure also shows the energy deposition in a bare scintillator and with only the lead pig. Each of the configurations shows a sharp turn on time and a pulse 1-ns wide. The initial rise occurs when

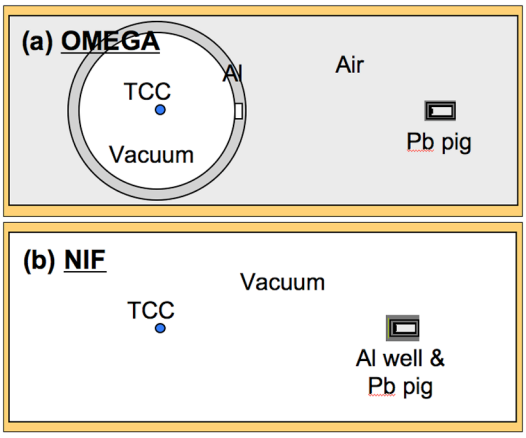

FIG. 3. Monte Carlo geometries used to calculate energy deposition rate in detector scintillator. Border represents edge of problem, not room wall.

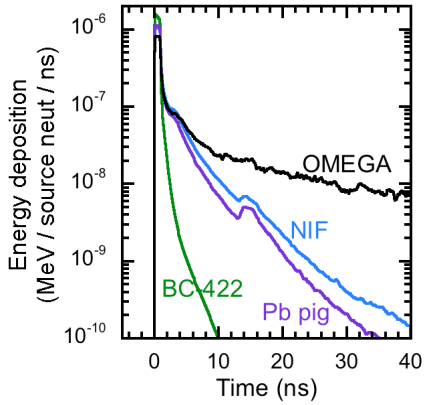

FIG. 4. Monte Carlo calculated energy deposition rate in detector scintillator for bare scintillator, with Pb pig, and in NIF and OMEGA configurations. Neutrons enter scintillator at time = 0.

the neutrons first enter the scintillator. The width corresponds to the transit time of the DD neutrons through the scintillator. In the case of the lead pig only, scattering from the lead produces the equivalent of about 3-ns exponential decay. Neutrons reflected from the back end of the lead pig cause an increase in the energy deposition rate 14 ns after neutrons first enter the scintillator. For the OMEGA configuration target chamber scattering produces a tail with the equivalent of a 24-ns decay rate. The NIF configuration with the addition of the aluminum well produces a scattering tail intermediate between the bare detector and the OMEGA configuration. At both facilities, more than 50% of the detected events are scattered neutrons.

The scintillator response for BC422 is the sum of exponential decays.[14] For these calculations only the primary 1.3-ns decay component is used. The recording system response was initially modeled and later experimentally measured with a short burst of x rays (~100 ps) interacting directly in the MCP portion of the PMT with the PMT photocathode-to-MCP gap gated off. The measured 1.3 ns FWHM pulse represents the combined response of the PMT, cables, and oscilloscope, but excludes the scintillator response (Fig. 5). Cosmic ray events detected in the PMT produced similar results.

Total system PRFs are obtained by convolving the three components together. Figure 6 shows PRFs plotted on semilog and linear scales for four different configurations. The bare scintillator shows the narrowest response of 4-ns FWHM. The other three configurations have a width of ~4.25 ns. After 8 ns the tails of the OMEGA and NIF PRFs start to diverge because of differences in target chamber and well scattering. Each response function differs only in the neutron energy deposition rate in the

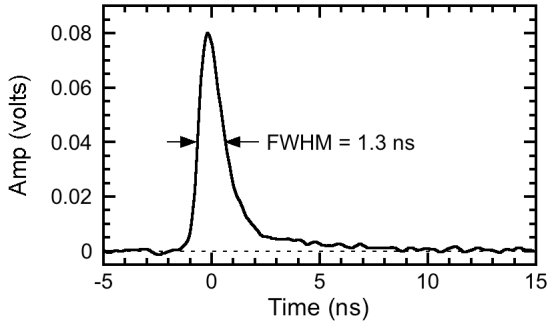

FIG. 5. Measured recording system response to x rays interacting in MCP section of PMT. Response includes effect of PMT, cables, and oscilloscope.

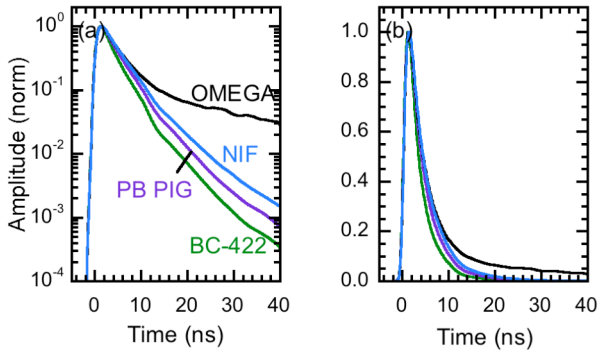

FIG. 6. System response functions. (a) Semilog scale. (b) Linear scale. Time base t = 0 adjusted to instant neutrons arrive at scintillator.

scintillator caused by the scattering environment.

V. nTOF MEASUREMENTS

Neutron yield, ion temperature, and bang time, the three basic nTOF measurements all begin with the same basic analysis: finding the best Gaussian pulse that represents the data. Estimating the best Gaussian is a relatively simple iterative process. First, a Gaussian pulse is selected with a width, amplitude and center time based on the recorded data. The Gaussian is convolved with the system PRF to form an estimate of the recorded signal. The process is repeated varying the Gaussian width, amplitude, and center time until the best least squares fit is obtained. To reduce the effect of slight errors in the tail of the PRF and late time scattering events in the recorded signal, the fit is done from the beginning of the pulse through the 50% point on the trailing edge of the pulse. Samples of least squares fits are shown in Fig. 7. It is clear the simple model of a spherical chamber fails at late times. The OMEGA target chamber has large mirror and lens structures to bring the 60 laser beams into the chamber. An estimate for scattering from these structures is added to Fig. 8a. This improves the fit at late time as seen in Fig. 9a. But because the scattering is caused by structures nearly 30 degrees off the TCC-detector axis, the entire effect is after the trailing 50% point for this data. While it clearly improves the apparent quality of the fit, it has no effect on the estimated width of the underlying Gaussian.

A. Temperature Measurements

To test the quality of the PRF generated for the OMEGA configuration, ion temperatures calculated with it are compared

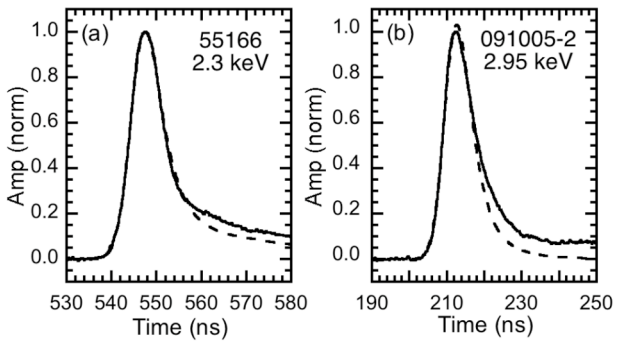

FIG. 7. Samples of fits to data using PRFs based on Monte Carlo scattering model. Solid lines are data, dashed lines are fits. (a) OMEGA calibration shot. (b) NIF shot.

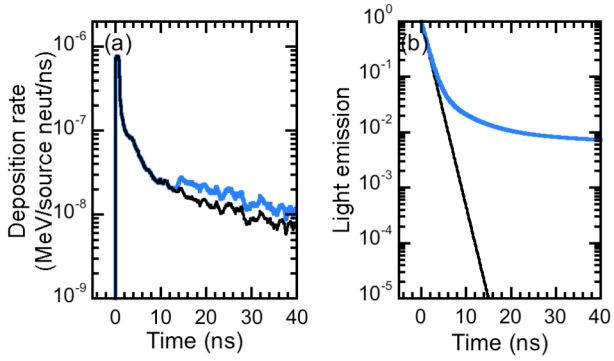

FIG. 8. Modifications made to the PRFs for better fits to late time scattering. (a) OMEGA change represents scattering from mirror structures, (b) Slight change in decay rate accounts for unknown NIF scattering source: τ_1 = 1.3 ns (96%), τ_2 = 6 ns (3%), τ_3 = 123 ns (1%).

with the standard parametric fit used by LLE. Figure 10 shows that the temperatures calculated by the two different methods produce nearly identical results. The ratio of temperatures over 6 calibration shots is 1.00 with a standard deviation of 3.7%.

Applying the NIF PRF to NIF data produces a fit that appears to have some error (see Fig 7b). An overlay of NIF and OMEGA shot data (Fig. 11) shows that there is additional NIF scattering that is not present at OMEGA. The leading edge and peak of the NIF and OMEGA pulses are nearly identical. But there is a significant bulge on the backside of the pulse beginning at the 60% level. Then late in time the NIF pulse remains high. This late time behavior is consistent from shot to shot. The PRF needs to account for the additional scattering. A significantly improved fit is achieved by adding small amounts of longer scintillator decay components (Fig. 8b). Figure 9b shows the improved fit using 96%, 3% and 1% of decay rates of 1.3, 6.0, 123 ns respectively. Figure 12 shows a comparison of the temperatures recorded by two of the nTOF detectors. A ratio of the temperatures shows that they agree with each other from shot-to-shot with a standard deviation of 7.9% per detector.

B. Yield Measurements

Calibrations for the NIF nTOF detector yield sensitivities were determined at the OMEGA facility where target yields are routinely measured by absolutely calibrated OMEGA yield detectors.[15] Signals were recorded for exploding pusher targets yielding 10^8 to 10^{10} DD neutrons. Transferring detector sensitivity from OMEGA to NIF is a straightforward process.

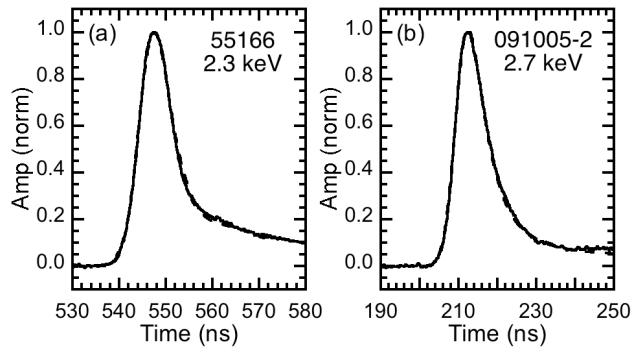

FIG. 9. Examples in Fig. 7 with improved fits using slightly modified PRFs. Solid lines are data, dashed lines are fits. (a) OMEGA calibration shot. (b) NIF shot.

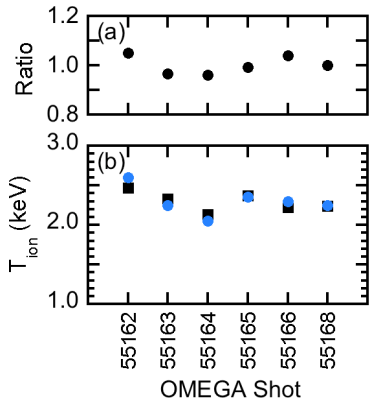

FIG 10. OMEGA temperature comparison. (a) Ratio vs shot. (b) T_{ion} vs shot number. Circles are PRF fit, squares are LLE fit.

The nTOF detector sensitivity at NIF (in the absence of scattering) is the sensitivity as determined at OMEGA corrected for facility differences in detector distance from TCC and the neutron transmission between TCC and the detector. A slight additional adjustment to the calibration is required because of the different neutron scattering properties of the two facilities. Figure 4 shows the neutron energy deposition rate in the scintillator at the two facilities. These rates include the effect of distance from TCC, neutron transmission, and scattering. Figure 13 shows the integral of the energy deposition rates. The Omega integral is shown at a distance of 5.2 m and corrected to 4.58 m. The NIF integral is for the detector at 4.58 m. The difference in the NIF and OMEGA integrals is the correction that needs to be made to the OMEGA derived calibration. Total correction is about 10% for pulse widths on order of 10 ns.

Neutron yields were measured with two similar nTOF detectors, one calibrated at OMEGA, the other initially uncalibrated. During the course of the NIF experiments, the second detector was calibrated against the first. Figure 14 shows the ratio of the yields recorded by the two detectors for DD neutron yields ranging from $8x10^8$ to $2x10^{10}$. The standard deviation for the ratio is 5.62%. Dividing by the square root of two gives the standard deviation for a single detector as 4%.

C. Bang Time Measurements

Although the first nTOF detectors are not ideal for making bang time measurements, an effort was made to estimate the quality of future bang time measurements. Neutron bang time

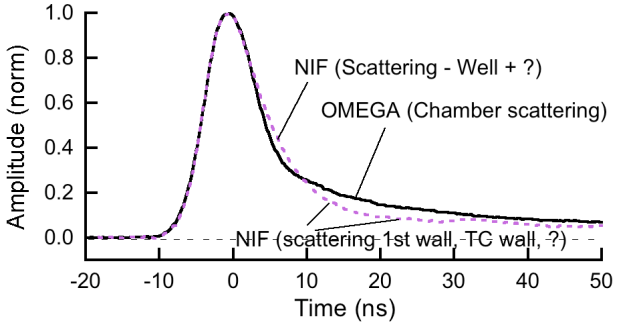

FIG. 11. Overlay of average OMEGA and NIF pulses for similar yields and temperatures. OMEGA (solid line - 6 shot average), NIF (dotted line - 9 shot average). Trailing edge of pulses show scattering induced differences between signals.

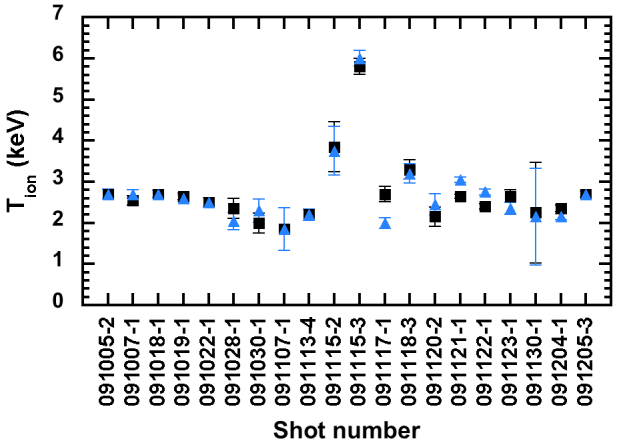

Fig 12. Comparison of NIF ion temperatures recorded by two different nTOF detectors.

measurements are best made when the recorded pulse has the narrow width. An optimized system would have a fast detector using a quenched scintillator with nonreflecting surfaces and a short path between TCC and the detector to reduce temperature induce pulse broadening. Ideally, DT neutrons with a factor of 6 less time spread would be used instead of DD neutrons. The standard nTOF analysis produces a time for the measured pulse. By referencing the neutron pulse to a fiducial pulse simultaneously recorded with the data, the neutron pulse can be timed relative to the incident laser pulse. For this exercise, the two nTOF signals were related to each other. Any jitter between the signals is an indication of the jitter expected in a bang time measurement. Figure 15 shows the time difference between the neutron signals crossed timed with the fiducial after a constant time is subtracted. The measured time jitter between the two detectors is 360 ps. The jitter associated with a single detector is 255 ps. The expected jitter is on the order of 175 ps. This estimate is based on the neutron statistics and does not include the effect of signal noise and the 100 ps sample spacing. The DD neutron pulses are ~6 ns wide and have ~5000 detected neutrons (at 10^{10} yield), and a pulse height derating factor of ~2. Jitter = (2 x 6) / $(5000)^{1/2}$ ns.

VI. SUMMARY

The first three of eighteen nTOF channels have been installed and operated successfully at the NIF during the first target campaign to use all 192 NIF beams. Some of the targets were filled with up to 10% deuterium to produce ~10^{10} DD

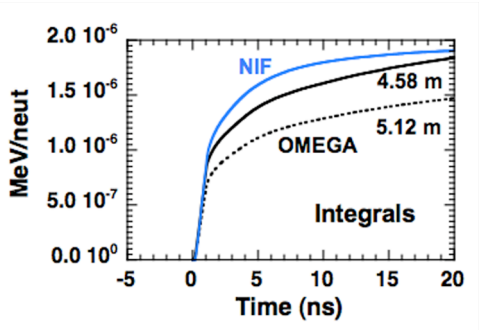

Figure 13. Comparison of total energy deposition versus time in scintillator at NIF and OMEGA.

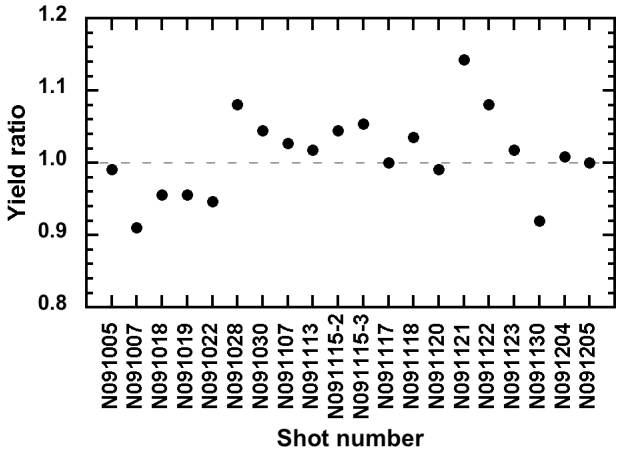

Fig 14. Ratio of NIF neutron yields measured by two independent detectors.

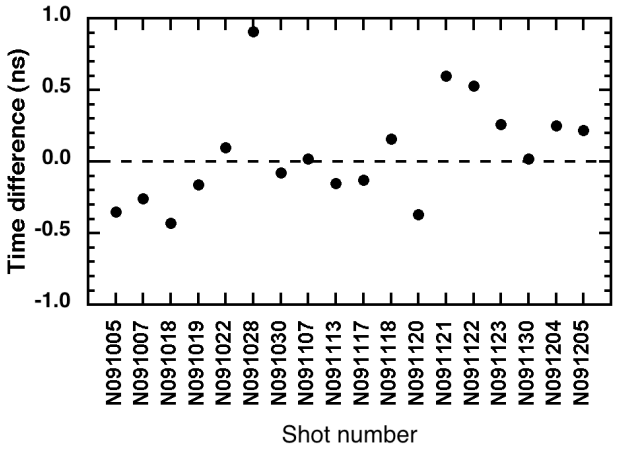

FIG. 15. Difference in NIF bang time recorded by two independent detectors.

neutrons for diagnostic testing. The detectors used in this work were designed to operate in the presence of large bursts of target x rays. Lead shielding provided attenuation of the prompt x-ray pulse. To provide scientists and engineers with early test data, these detectors were used to measure yield, ion temperature, and bang time even though detector position and configuration was not ideal for temperature or bang time measurements.

For each measurement, signal analysis starts with finding the best Gaussian that corresponds with the recorded signal. The three Gaussian parameters (amplitude, FWHM, and peak time) are related to the three measurements: yield (proportional to amplitude x FWHM), temperature (proportional to square of the FWHM) and bang time (shifts with peak time). Finding the best Gaussian requires a good knowledge of the system PRF (impulse response). With the heavily shielded detectors more than 50% of the signal comes from scattered neutrons. The OMEGA and NIF PRFs differ because of their different neutron scattering environments. A combination of Monte Carlo simulations and detector characterizations were used to construct an appropriate response function for each of the two facilities.

The quality of the generated OMEGA PRF is demonstrated by examining temperatures obtained from the OMEGA calibration shots. Temperatures obtained using the generated PRF were compared with temperatures found using the standard OMEGA method employing a set of fit parameters to describe the PRF. The 3.7% variation between temperatures shows the two PRFs produce essentially the same result for OMEGA data.

A slight difference in pulse shape is evident when NIF and OMEGA signals are compared. NIF has additional scattering sources that cause a slight bump on the back side of the pulse and prevent the pulse from returning to base line. Analysis with the NIF specific PRF instead of the OMEGA generated PRF produces good results.

NIF nTOF signal quality is very good with low noise. Data were collected on four scope channels along with a good fiducial pulse. Comparison of measurement results between two nearly identical detectors showed yield precision to be 4%, temperature precision to be 7.9% and bang time jitter to be 255 ps. These early measurements support our belief that the full set of nTOF detectors will produce excellent measurements of neutron yield, temperature, and bang time. Yield precision at 4% has been demonstrated. The collimated nTOF detectors at 20 m will record clean DT neutron signals with ~ 5 ns widths at 4 keV. With widths measured with 150-ps accuracy, temperature precision of ~5% is expected. The detector configurations at NIF were far from optimal for making bang times measurements. Yet they are the source of an optimistic prediction for the precision of the planned 4.5-m CVD diamond based nTOF detectors. With a temporal spread of ~1.1 ns at the detector, the estimated bang time jitter for DT neutrons is 30 ps. The NIF nTOF system is expected to produce high quality measurements of yield, ion temperature, and bang time for future NIF experiments.

ACKNOWLEDGMENT

This work performed under the auspices of the U.S. Department of Energy by Lawrence Livermore National Laboratory under Contract DE-AC52-07NA27344.

[1]V. Yu. Glebov, D. D. Meyerhofer, T. C. Sangster, C. Stoeckl, S. Roberts *et al.*, Rev. Sci. Instrum. **77**, 10E715 (2006).
[2] E. Moses, R. Boyd, B. Remington, C. Keane, and R. Al-Ayat, Phys. Plasmas **16**, 041006 (2009).
[3] N. B. Meezan, L. J. Atherton, D. A. Callahan, E. L. Dewald, S. Dixit *et. al.*, Phys. Plasmas **17**, 056304 (2010).
[4] V. Yu. Glebov, C. Stoeckl, T. C. Sangster, S. Roberts, G. J. Schmid, R. A. Lerche, and M. J. Moran, Rev. Sci. Instrum. **75**, 3559 (2004).
[5] R. A. Lerche and B. A. Remington, Rev. Sci. Instrum. **61**, 3131 (1990).
[6] R. A. Lerche, D. R. Kania, S. M. Lane, G. L. Tietbohl, C. K. Bennett, and G. P. Baltzer, Rev. Sci. Instrum. **59**, 1697 (1988).
[7] H. Brysk, Plasma Phys. **15**, 611 (1973).
[8] R. A. Lerche, D. W. Phillion, and G. L. Tietbohl, Rev. Sci. Instrum. **66**, 933 (1995).
[9] L. Disdier, A. Rouyer, I. Lantuéjoul, O. Landoas, J. L. Bourgade, T. C. Sangster, V. Yu. Glebov, and R. A. Lerche, Phys. Plasmas **13**, 056317 (2006).
[10]R. A. Lerche, L. W. Coleman, J. W. Houghton, D. R. Speck, and E. K. Storm, Appl. Phys. Lett. **31**, 645 (1977).
[11]G. J. Schmid, R. L. Griffith, N. Izumi, J. A. Koch, R. A. Lerche, M. J. Moran, T. W. Phillips, R. E. Turner, V. Yu. Glebov, T. C. Sangster, and C. Stoeckl, Rev. Sci. Instrum. **74**, 1828 (2003).
[12]T. J. Murphy, R. E. Chrien, and K. A. Klare, Rev. Sci. Instrum. **68**, 610 (1997).
[13]TART2005 Monte Carlo Code, distributed by Radiation Safety Information Computational Center, P.O. Box 2008, Oak Ridge, TN 37831.
[14]C. A. Barrera, Ph.D. Thesis, University of California at Berkeley (2007).
[15]M. J. Moran, V. Yu. Glebov, C. Stoeckl, R. Rygg and Brook-Eden Schwartz, Rev. Sci. Instrum. **76**, 023506 (2005).